Analytic estimation and minimization of line edge roughness in electron-beam lithography

Rui Guo, Soo-Young Lee, Jin Choi, Sung-Hoon Park, In-Kyun Shin, and Chan-Uk Jeon

Citation: Journal of Vacuum Science & Technology B **33**, 06FD07 (2015); doi: 10.1116/1.4936070
View online: http://dx.doi.org/10.1116/1.4936070
View Table of Contents: http://scitation.aip.org/content/avs/journal/jvstb/33/6?ver=pdfcov
Published by the AVS: Science & Technology of Materials, Interfaces, and Processing

Articles you may be interested in
Minimization of line edge roughness and critical dimension error in electron-beam lithography
J. Vac. Sci. Technol. B **32**, 06F505 (2014); 10.1116/1.4899238

Simulation of amine concentration dependence on line edge roughness after development in electron beam lithography
J. Appl. Phys. **104**, 024303 (2008); 10.1063/1.2952046

Local line edge roughness in microphotonic devices: An electron-beam lithography study
J. Vac. Sci. Technol. B **25**, 235 (2007); 10.1116/1.2426978

Electron-beam patterning with sub- 2 nm line edge roughness
J. Vac. Sci. Technol. B **23**, 271 (2005); 10.1116/1.1856466

Representation of nonrectangular features for exposure estimation and proximity effect correction in electron-beam lithography
J. Vac. Sci. Technol. B **22**, 2929 (2004); 10.1116/1.1824058

Redistribution subject to AVS license or copyright; see http://scitation.aip.org/termsconditions. Download to IP: 131.204.21.179 On: Thu, 19 Nov 2015 16:00:59

Analytic estimation and minimization of line edge roughness in electron-beam lithography

Rui Guo and Soo-Young Lee[a)]
Department of Electrical and Computer Engineering, Auburn University, Auburn, Alabama 36849

Jin Choi, Sung-Hoon Park, In-Kyun Shin, and Chan-Uk Jeon
Samsung Electronics, Photomask Division, 16 Banwol-Dong, Hwasung 445-701, Kyunggi-Do, Korea

(Received 28 June 2015; accepted 6 November 2015; published 19 November 2015)

As the feature size is reduced well below 100 nm, the line edge roughness (LER) will eventually become a resolution-limiting factor in the electron-beam (e-beam) lithography since the LER does not scale with the feature size. Therefore, it is essential to minimize the LER in order to achieve the highest resolution possible by the e-beam lithographic process. A simulation or experiment based method for minimizing the LER can be very time-consuming and expensive since repetitive simulations or experiments may be required. In this study, a new analytic model and a method for estimating the LER are developed based on the model, and an analytic procedure for minimizing the LER is also derived based on the new analytic model. In this new approach, the LER is derived from the distribution of the stochastic developing rate in the resist, which is assumed to be known. The results obtained by the analytic estimation method and the minimization procedure are shown to be close to those by the simulation method. The current work includes generalization of the results of this study with more practical models. © *2015 American Vacuum Society*.
[http://dx.doi.org/10.1116/1.4936070]

I. INTRODUCTION

Electron-beam (e-beam) lithography is widely employed in a variety of areas such as fabrication of photomasks, imprint lithography molds, experimental circuit patterns, etc., for its ability to transfer ultrafine features onto the resist.[1–4] Its two main limitations are the proximity effect caused by electron scattering and the low throughput due to the pixel-by-pixel or feature-by-feature writing. The importance of developing effective and efficient schemes for correcting the proximity effect has been well recognized for a long time, and various methods were proposed and implemented by many researchers.[5–8] As the feature size continues to be reduced, the line edge roughness (LER) will eventually become a resolution-limiting factor in the e-beam lithography since the LER does not scale with the feature size.[9] Therefore, it is essential to minimize the LER in order to achieve the highest resolution possible by the e-beam lithographic process.

Many of the previous efforts made to reduce the LER are based on an empirical or trial-and-error approach via experiment or simulation.[10–12] However, such a method can be very time-consuming and expensive since repetitive simulations or experiments may be required. In order to avoid the simulation and experiment, one may take an analytic approach for estimating and minimizing the LER. In the efforts to estimate the effects of the LER on the device behaviors,[13,14] theoretical models were formulated; however, an analytic expression of the LER was not derived. In another study,[15] a comprehensive stochastic model of LER was formulated with approximate expressions of the standard deviation of the final deprotection level of polymer molecules in the resist. An infinite contrast of development process was assumed to obtain the LER directly from the blocked polymer latent image without modeling the development process. In our previous analytic method of estimating the LER,[16] the final expression of the LER is not derived as a function of the e-beam lithographic parameters such as dose, etc. Therefore, it is not suitable for the analytic procedure of minimizing the LER with respect to those parameters.

In this study, a new analytic method for estimating the LER at any layer of resist has been developed for the case where a long single line is exposed with a uniform dose. Without having to obtain and refer to the remaining resist profile, the (mathematical expression of) LER is derived explicitly from the stochastic fluctuation of the developing rate distribution on which the remaining resist profile mainly depends. The stochastic fluctuation of developing rate comes from the randomness in both energy deposition process (electron scattering) and electron influx (shot noise) and may be determined from the stochastic point spread function and shot noise model. Also, an analytic procedure for minimizing the LER with respect to the dose has been developed with all the other e-beam lithographic parameters, i.e., beam energy, developing time, etc., fixed. It should be pointed out that even though the current study focuses on the stochastic variation of the developing rate, it is expected that other factors can be considered under this model, by adjusting the stochastic developing rate to reflect their direct or equivalent effects on the developing rate. For example, to consider the randomness in the developing process, an additional fluctuation may be added to the developing rate. The current and future work includes generalization of the analytic model, e.g., allowing the spatially varying dose, reduction of the feature area to be exposed, and consideration of other stochastic factors, where the analytic estimation and minimization methods described in this paper are expected to be applicable.

a)Electronic mail: leesooy@eng.auburn.edu

Redistribution subject to AVS license or copyright; see http://scitation.aip.org/termsconditions. Download to IP: 131.204.21.179 On: Thu, 19 Nov 2015 16:00:59

The rest of the paper is organized as follows. The analytic estimation of the LER is described in Sec. II. The procedure for minimizing the LER is presented in Sec. III. The procedure for estimating the LER through the simulation is described in Sec. IV. The results of estimating and minimizing the LER are discussed in Sec. V, followed by a summary in Sec. VI.

II. ANALYTIC ESTIMATION OF LER

In this section, the LER is analytically estimated as a function of the edge location with the dose fixed at a certain level D and therefore D is not explicitly considered in the estimation procedure. However, in Sec. III where the LER is minimized with respect to the dose level D which is a variable will be explicitly considered.

A. Analytic model

A three-dimensional (3D) model of substrate system is employed in this study. As shown in Fig. 1(a), a resist layer is on the top of the substrate where the X-Y plane corresponds to the top surface of resist, and the resist depth is along Z-dimension. A long line feature, which is W nm wide in the X-dimension and L nm long in the Y-dimension [see Fig. 1(b)], is exposed with a uniform dose D, and its right edge is along the Y axis, i.e., x is negative inside the feature and positive outside. The LER at varying mean edge location (x) in a resist layer ($z = z_0$) is to be derived from the (stochastic) developing rate, which is denoted by $R(x, y, z)$. The mean and variance of $R(x, y, z)$ are denoted by $m_R(x, y, z)$ and $\sigma_R^2(x, y, z)$, respectively. And $m_R(x, y, z)$ and $\sigma_R^2(x, y, z)$ averaged along the Y-dimension are expressed as $m_R(x, z)$ and $\sigma_R^2(x, z)$, respectively.

Given a distribution of the developing rate, the remaining resist profile is determined through the resist development process. The proposed analytic method for estimating the LER follows the resist development process while it does not derive the remaining resist profile. Assume that the resist development process can be modeled by "development paths" where a development path is defined as a path along which resist is developed, as illustrated in Fig. 2. Each development path starts from the resist surface toward the boundary of resist profile. Given a possible edge location x, the development path which takes the minimum time to reach the location from the top surface of resist is defined as the "dominant path," and its length is denoted by s. Note that the LER is proportional to the length fluctuation of the dominant path of an edge location. The developing rate along the dominant path is expressed by $R(p)$, where $0 \le p \le s$, as shown in Fig. 3. The fluctuation of the time taken by the dominant path is derived first, and then, it is used to derive the fluctuation of the dominant-path length, which is eventually converted into the LER at the edge location.

Below is a summary of the notations:

(1) $R(p)$: resist developing rate at p on the dominant path.
(2) $m_R(p)$: mean of developing rate at p on the dominant path.

(a)

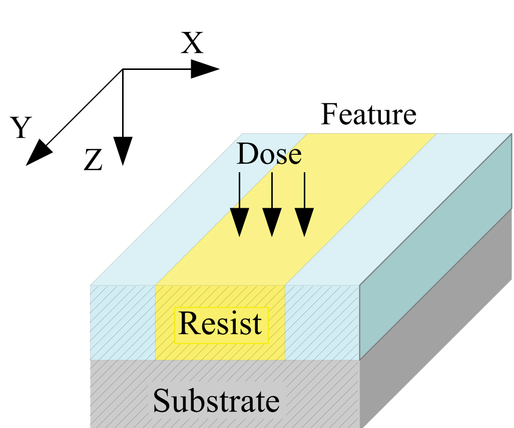

(b)

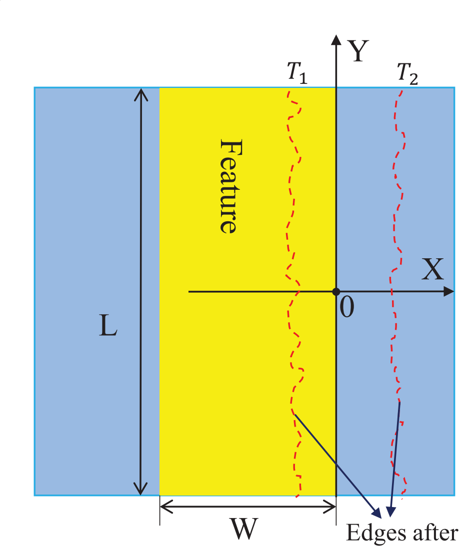

FIG. 1. (Color online) (a) 3D model of substrate system and (b) a line feature of size $W \times L$ with its right edge on the Y-axis. After the development process, the boundary (edge) of remaining resist profile can be inside ($x < 0$) or outside ($x > 0$) the feature. For example, the two dashed lines may represent the two possible edges for two different developing times, T_1 and T_2, where $T_1 < T_2$.

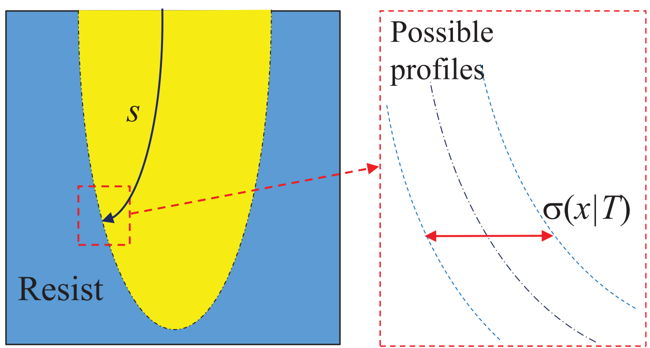

FIG. 2. (Color online) Development path in the resist and the variation of edge location with a fixed developing time.

Redistribution subject to AVS license or copyright; see http://scitation.aip.org/termsconditions. Download to IP: 131.204.21.179 On: Thu, 19 Nov 2015 16:00:59

(3) $\sigma_R(p)$: standard deviation of developing rate at p on the dominant path.
(4) T: developing time.
(5) D: uniform-dose level.

B. Estimation procedures

The LER is defined as the variation of the edge location at a layer of the remaining resist profile, as shown in Fig. 2, and is quantified as the standard deviation of the edge location x measured in the lateral dimension given a developing time T, i.e.,

$$\text{LER} = \sigma(x|T). \quad (1)$$

Derivation of the analytic expression of the LER is carried out in three steps: (1) given an edge location x_0 at a layer (z_0), at which the LER is to be estimated, find the dominant path to reach the location, and derive the fluctuation of the developing time T taken by the dominant path, (2) estimate the direction of the dominant path at the edge location x_0, and (3) derive the expression of the LER given a developing time T.

1. Dominant path and the fluctuation of developing time

The edge location is determined by the dominant path of the location. To estimate the LER at an edge location (x_0, z_0), its dominant path needs to be found first. From the distribution of developing rate, the total developing time taken by each development path can be calculated. Since the developing process is isotropic, it is not easy to derive the dominant path analytically in one step. An iterative method is used to derive the dominant path (see Fig. 4).

In the first step, the iterative method traces back from the edge location to the top surface of the resist. For example, given the edge location (x_0, z_0), the point (x_1, z_1) that takes the minimum developing time from (x_0, z_0) to (x_1, z_1) among all possible x_1, where $z_1 < z_0$, is found. From (x_1, z_1), the next point (x_2, z_2) can be derived by the same procedure. Repeating this procedure until $z_i = 0$ which corresponds to the top surface of the resist. Then, $[(x_0, z_0), (x_1, z_1), (x_2, z_2), \ldots]$ represents a possible development path to (x_0, z_0). Note that even though the developing time between two adjacent points on the path is the minimum, the total developing time of this path may not be the minimum among all possible paths. Therefore, in the second step, with (x_0, z_0) fixed, additional possible paths are found by adjusting each of the remaining points and tracing back from the point as in the first step. Of all the derived paths, the path that takes the minimum total developing time is used as the dominant path.

The fluctuation of developing time can be directly derived from the developing rate fluctuation on the dominant path. Given $R(p)$ on the dominant path, the developing time T is expressed as the integral of $1/R(p)$ along the path

$$T = \int_{p=0}^{s} \frac{dp}{R(p)}. \quad (2)$$

Assuming that the correlation of $1/R(p)$ at any two points (p_1, p_2) on the dominant path denoted as $Cov_{1/R}(p_1, p_2)$ is known, the variance of developing time is derived as

$$\sigma^2(T|s) = \int_{p=0}^{s} \sigma^2_{\frac{1}{R}}(p)dp + \int_{p_1=0}^{s}\int_{p_2=0}^{s} Cov_{\frac{1}{R}}(p_1, p_2)dp_2dp_1. \quad (3)$$

2. Direction of the development path

The direction of the resist development is normal to the surface of remaining resist profile and is not always lateral. Therefore, the variation of the dominant-path length may not be quantitatively the same as the LER to be measured in the lateral dimension (X-dimension), as shown in Fig. 5. The

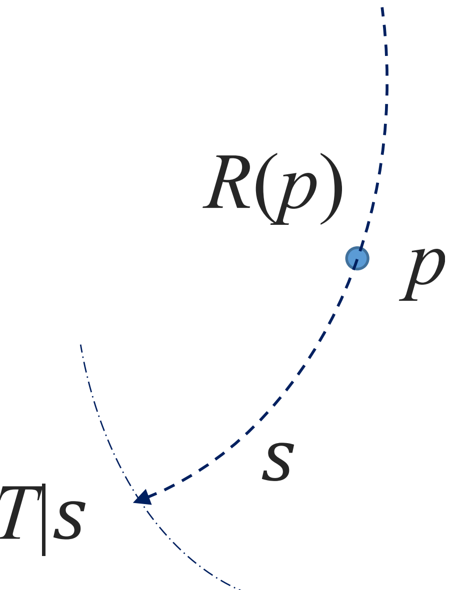

FIG. 3. (Color online) Developing rate $R(p)$ at a point p on a development path of which the length is denoted by s.

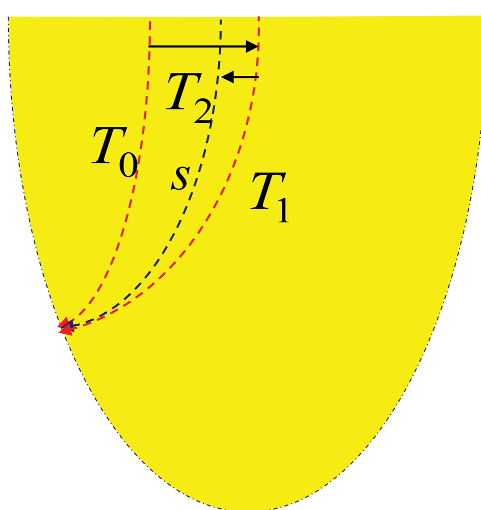

FIG. 4. (Color online) Dominant path is the development path taking the least amount of time to reach an edge location, x.

Redistribution subject to AVS license or copyright; see http://scitation.aip.org/termsconditions. Download to IP: 131.204.21.179 On: Thu, 19 Nov 2015 16:00:59

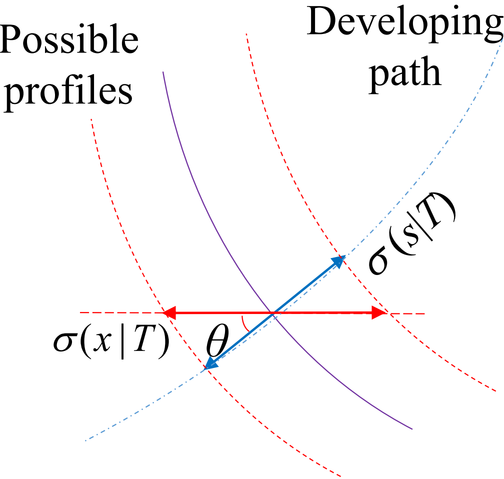

FIG. 5. (Color online) Fluctuation of the dominant-path length is projected onto the X (lateral) dimension.

direction of the development path is expressed as the angular deviation θ from the lateral direction and needs to be derived to obtain an accurate estimation of the LER.

To facilitate the derivation of θ, the resist development process is modeled by "L-shape" paths.[17] Each L-shape path starts from the resist surface toward the boundary of resist profile, consisting of a vertical path segment (which represents the vertical development of resist) and a lateral path segment (which represents the lateral development of resist). It has been shown that the remaining resist profiles estimated using L-shape paths are as accurate as those by the cell removal and fast marching methods.[17]

In the region close to the feature edge, the resist development usually progresses both laterally and vertically. On the other hand, the resist development progresses mostly vertically in the region sufficiently away from the feature edge. Let x_B represent the boundary between the two regions.

For a possible edge location close to the feature edge ($x \le x_B$), the L-shape path starting from $(x_B, 0)$ is the dominant path on the X-Y plane ($z = z_0$), and the remaining resist profile derived by such L-shape path is shown in Fig. 6(a). On the adjacent X-Y plane ($z = z_0 + dz$), assuming that the dominant path has the same vertical segment when dz is small, the angle θ is derived as

$$\theta = \tan^{-1}\left(\frac{dx}{dz}\right) = \tan^{-1}\left(\frac{m_R(x, z_0)\cdot \Delta T_1}{m_R(x_B, z_0 + dz)\cdot \Delta T_2}\right), \quad (4)$$

where ΔT_1 is the difference of the developing time between the two dominant paths in the lateral dimension, and ΔT_2 is that in the vertical dimension as illustrated in Fig. 6(a). Since the two paths take the same total developing time and share the segments, which also take the same amount of developing time except ΔT_1 and ΔT_2, ΔT_1 is equal to ΔT_2 when dz is close to 0. The angle θ is simplified to

$$\theta = \tan^{-1}\left(\frac{m_R(x, z_0)}{m_R(x_B, z_0)}\right). \quad (5)$$

(a)

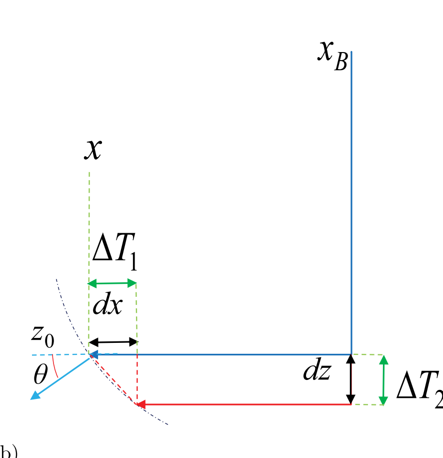

(b)

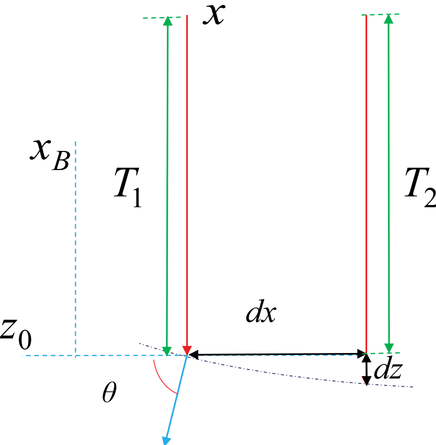

FIG. 6. (Color online) Direction of development path in a region (a) close to the feature edge and (b) close to the feature center.

For an edge location close to the feature center ($x > x_B$), the dominant L-shape path can be approximated to consist of only a vertical segment, as shown in Fig. 6(b). The angle θ is derived as

$$\theta = \tan^{-1}\left(\frac{dx}{dz}\right). \quad (6)$$

Since the two paths take the same total developing time, the following relationships are derived:

$$T_1 = \int_{z=0}^{z_0} m_{\frac{1}{R}}(x, z)dz, T_2 = \int_{z=0}^{z_0} m_{\frac{1}{R}}(x + dx, z)dz,$$
$$T_1 = T_2 + dz \cdot m_{\frac{1}{R}}(x + dx, z_0). \quad (7)$$

From Eq. (7), when dz is close to 0, the angle θ is simplified to

$$\theta = \tan^{-1}\left(\frac{dx}{dz}\right) = \tan^{-1}\left(\frac{m_{\frac{1}{R}}(x, z_0)}{\int_0^{z_0} \frac{\partial m_{\frac{1}{R}}(x, z)}{\partial x} dz}\right). \quad (8)$$

Redistribution subject to AVS license or copyright; see http://scitation.aip.org/termsconditions. Download to IP: 131.204.21.179 On: Thu, 19 Nov 2015 16:00:59

In the region close the feature edge, the θ evaluated by Eq. (5) is larger than that by Eq. (8) since the developing rate varies fast in the lateral dimension. On the other hand, in the region close to the feature center, the θ by Eq. (8) is larger than that by Eq. (5). Therefore, in this study, instead of deriving x_B analytically which is not straightforward, the θ is evaluated with the approximation of $m_R(x_B, z_0) \approx m_R(W/2, z_0)$ as follows:

$$\theta = \max\left(\tan^{-1}\left(\frac{m_R(x,z_0)}{m_R\left(\frac{W}{2},z_0\right)}\right), \tan^{-1}\left(\frac{m_{\frac{1}{R}}(x,z_0)}{\int_0^{z_0}\frac{\partial m_{\frac{1}{R}}(x,z)}{\partial x}dz}\right)\right). \tag{9}$$

3. LER at a layer

The fluctuation of the dominant-path length (s given T) may be related to the fluctuation of developing time taken by this path. If the developing rate is constant (R), the fluctuation of developing time can be directly converted into the fluctuation of s given T as

$$\sigma(s|T) = \sigma(T|s)\cdot R. \tag{10}$$

In reality, the developing rate varies spatially and is stochastic at each point. However, it would be a reasonable approximation that the developing rate around s is represented by the mean of the developing rate at s, i.e., $m_R(s)$ (refer to Fig. 7). Then, a more realistic relationship between $\sigma(s|T)$ and $\sigma(T|s)$ can be expressed as

$$\sigma(s|T) = \sigma(T|s)\cdot m_R(s). \tag{11}$$

Since the LER is measured in the lateral dimension (X-dimension), $\sigma(s|T)$, which is derived along the direction of development path, needs to be projected onto the X-dimension to get the LER (see Fig. 5)

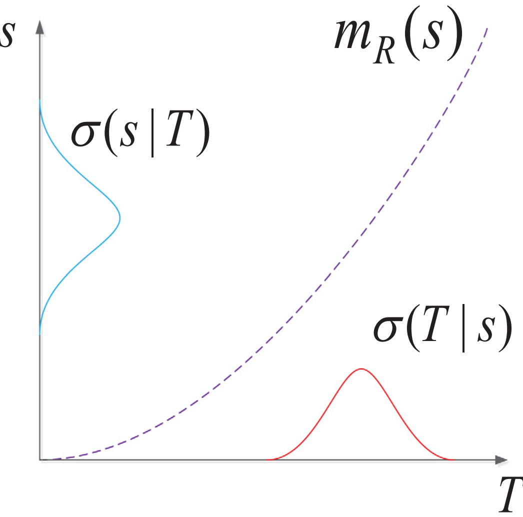

FIG. 7. (Color online) $\sigma(s|T)$ is derived from $\sigma(T|s)$ through the mean of developing rate ($m_R(s)$).

$$\sigma(x|T) = \frac{\sigma(T|s)\cdot m_R(s)}{\cos(\theta)}. \tag{12}$$

It needs to be pointed out that the interaction between adjacent development paths is not taken into account in the above derivation. The interaction tends to decrease the variation (of path length) among the paths and reduces the LER. Therefore, an adjustment factor[16] is employed to compensate the interaction between paths, and the final expression of LER [from Eqs. (3) and (12)] is given as

$$\sigma(x|T) = \frac{\rho_T(s)+1}{2}\cdot\frac{\sqrt{\left(\int_{p=0}^{s}\sigma^2_{\frac{1}{R}}(p)dp + \int_{p_1=0}^{s}\int_{p_2=0}^{s}Cov_{\frac{1}{R}}(p_1,p_2)dp_2dp_1\right)}\cdot m_R(s)}{\cos(\theta)}. \tag{13}$$

III. ANALYTIC MINIMIZATION OF LER

An analytic procedure of minimizing the LER based on Eq. (13) is described in this section. In this study, the LER is minimized with respect to the dose which is uniformly applied to the entire area of a feature. The optimal edge location is first derived without explicitly involving the dose, and then, the optimal dose is related to the optimal edge location.

A. Optimal path length

As the dose increases, the edge location moves from the inside of a feature to the outside. Inside an exposed area of a feature, the LER decreases rapidly toward the boundary of the exposed area.[12] It continues to decrease over the boundary and right outside the exposed area, and then almost levels off or slightly increases in some cases. Therefore, the LER is not minimal at the feature boundary (where the critical dimension (CD) error is minimal, i.e., zero) in general. That is, the LER and CD error cannot be minimized at the same time (the same edge location or equivalently the same dose). Both the CD error and the LER need to be included in a cost function. The cost function employed in this study is

$$C(x) = \text{CD error} + 3\cdot\text{LER} = |x - x_t| + 3\cdot\text{LER}(s), \tag{14}$$

Redistribution subject to AVS license or copyright; see http://scitation.aip.org/termsconditions. Download to IP: 131.204.21.179 On: Thu, 19 Nov 2015 16:00:59

where x_t is the target edge location and its corresponding path length is s_t.

In this paper, the CD error is defined as the distance from the target edge location to the average (actual) edge location and the LER as the standard deviation of edge location (i.e., 1–σ LER). Hence, the cost function of $\text{CD error} + 3 \cdot \text{LER}$ may be considered practically as the worst case deviation of edge location from the target location (e.g., 99.7% in the case of Gaussian distribution). Also, $3 \cdot \text{LER}$ corresponds to the 3–σ LER typically used in the research and industry communities.

When $x < x_t$, i.e., inside the feature, both the LER and the CD error decrease as x increases. Therefore, the optimal x cannot be inside the feature. When $x \geq x_t$,

$$C(x) = x - x_t + 3 \cdot \text{LER}(s). \tag{15}$$

Around the target edge location x_t, the remaining resist profile is almost vertical and, therefore,

$$\theta(s) \approx 0,\ \cos\theta(s) \approx 1,\ \rho_T(s) \approx \rho_T(s_t), \tag{16}$$

$\sigma(T|s)$ changes very slowly around s_t

$$\sigma(T|s) \approx \sigma(T|s_t) = \sqrt{\left(\int_{p=0}^{s_t} \sigma^2_{\frac{1}{R}}(p)dp + \int_{p_1=0}^{s_t}\int_{p_2=0}^{s_t} Cov_{\frac{1}{R}}(p_1,p_2)dp_2dp_1\right)}. \tag{17}$$

From Eqs. (16) and (17), the LER [Eq. (13)] around x_t may be expressed as

$$\text{LER}(x) = \frac{\rho_T(s_t)+1}{2} \cdot \sigma(T|s_t) \cdot m_R(s). \tag{18}$$

Assuming that the cost function is a simple convex function, the optimal edge location s_{opt} is obtained from

$$\frac{dC(s)}{ds} = 1 + \frac{3\left(\rho_T(s_t)+1\right)}{2} \cdot \sigma(T|s_t) \cdot m'_R(s) = 0, \tag{19}$$

where $m'_R(s)$ is the first order derivative of the mean developing rate with respect to s. The optimal edge location s_{opt} is derived as

$$s_{\text{opt}} = m'^{-1}_R\left(\frac{2}{3\left(\rho_T(s_t)+1\right) \cdot \sigma(T|s_t)}\right), \tag{20}$$

where $m'^{-1}_R(\,)$ is the inverse function of $m'_R(\,)$.

B. Optimal dose

From this point on, the dose D is considered explicitly, which affects the developing rate. Let $m_{1/R}(s,D)$ denote the mean of $1/R$ at s when the dose is D. D_t and D_{opt} are the doses required to reach s_t and s_{opt} in T, respectively. Note that $D_{\text{opt}} > D_t$ since $s_{\text{opt}} > s_t$. In order to relate the optimal dose to the optimal edge location, the developing time, ΔT, taken by the dominant path to go from s_t to s_{opt} when $D = D_{\text{opt}}$ is computed. Since T is the same for both D_t and D_{opt}, ΔT must be equal to the change (decrease) in the developing time required to reach s_t when the dose is changed (increased) from D_t to D_{opt}.

$$\Delta T = \int_{s=s_t}^{s_{\text{opt}}} m_{\frac{1}{R}}(s, D_{\text{opt}})ds = s_t \cdot \left(\bar{m}_{\frac{1}{R}}(D_t) - \bar{m}_{\frac{1}{R}}(D_{\text{opt}})\right), \tag{21}$$

where $\bar{m}_{1/R}(D)$ is defined as $\frac{1}{s_t}\int_{s=0}^{s_t} m_{1/R}(s,D)ds$, i.e., the average time required to develop a unit length of resist.

The relationship between the dose and developing rate is nonlinear, and therefore, $\bar{m}_{1/R}(D)$ is a nonlinear function of D. However, a first-order approximation may be employed to evaluate Eq. (21). That is,

$$s_t \cdot \left(\bar{m}_{\frac{1}{R}}(D_t) - \bar{m}_{\frac{1}{R}}(D_{\text{opt}})\right) \approx s_t \cdot \bar{m}'_{\frac{1}{R}}(D_t) \cdot (D_{\text{opt}} - D_t), \tag{22}$$

where $\bar{m}'_{1/R}(\,)$ is the first-order derivative of $\bar{m}_{1/R}(\,)$ with respect to D.

As an approximation, ΔT may be computed with $D = D_t$ instead of $D = D_{\text{opt}}$ in Eq. (21), i.e., $\int_{s=s_t}^{s_{\text{opt}}} m_{1/R}(s,D_{\text{opt}})ds \approx \int_{s=s_t}^{s_{\text{opt}}} m_{1/R}(s,D_t)ds$. Then,

$$\int_{s=s_t}^{s_{\text{opt}}} m_{\frac{1}{R}}(s,D_t)ds = s_t \cdot \bar{m}'_{\frac{1}{R}}(D_t) \cdot (D_{\text{opt}} - D_t). \tag{23}$$

From Eq. (23), the optimal dose is derived as

$$D_{\text{opt}} = \frac{\int_{s=s_t}^{s_{\text{opt}}} m_{\frac{1}{R}}(s,D_t)ds}{s_t \cdot \bar{m}'_{\frac{1}{R}}(D_t)} + D_t. \tag{24}$$

Note that D_{opt} can be computed given the distribution of developing rate in the resist.

IV. SIMULATION

In order to verify the accuracy of the proposed analytic methods, the estimation and minimization results are compared with those obtained through the simulation. For the simulation, a set of stochastic point spread functions (PSFs) is generated for the substrate system of PMMA on Si using the software, CASINO, where the beam diameter is set to 3 nm and the density of PMMA to 1.18 g/cm^3. The stochastic exposure (electron energy deposited) distribution in the resist

Redistribution subject to AVS license or copyright; see http://scitation.aip.org/termsconditions. Download to IP: 131.204.21.179 On: Thu, 19 Nov 2015 16:00:59

is computed from the stochastic PSFs at the pixel interval of 1 nm, which is converted into the stochastic developing-rate distribution through a nonlinear mapping function determined from the experiment.[17] In this experiment, a single line is exposed with a uniform dose, and after the resist development in methylisobutyl ketone:isopropyl alcohol (IPA) = 1:3 for 60 s and IPA for 40 s at 21 °C, the depth in the cross-section of the remaining resist profile is measured at the center of line. By comparing the depth and its corresponding dose level, the mapping function is derived. The remaining resist profile is obtained through a development simulation using the path-based method developed earlier.[17] The development simulation is stopped at the developing time corresponding to the edge location at which the LER is to be evaluated. The LER is evaluated using the middle portion of line to exclude the end effects.

V. RESULTS AND DISCUSSION

A typical substrate system is employed, where a resist layer of PMMA with a certain thickness is on the top of the Si substrate. A single feature of size 90×400 nm ($W \times L$) is exposed with a uniform dose.

While the proposed analytic method can be applied to any layer of resist, the results for the bottom layer are provided since the LER is usually largest at the bottom layer. The LER computed from the analytic expression is compared with that obtained by the simulation for varying edge location (x), where $x = 0$ corresponds to the target edge location [see Fig. 1(b)]. The edge location is controlled by changing developing (development) time with the same exposure (developing rate) distribution. In the simulation, the development process continues until the boundary of developed feature reaches each edge location.

In Fig. 8(a), the results for the resist thickness of 300 nm, the beam energy of 50 keV, and the dose level of 640 μC/cm^2 are provided. It can be seen that the LER estimated by the analytic method is well matched with the LER by the simulation method. In Fig. 8(b), the results for a lower beam energy of 30 keV with the same dose are shown. Since the exposure is higher for 30 keV than 50 keV, for the same edge location, the developing time is shorter for 30 keV than for 50 keV. In Fig. 8(c), the results for a thinner thickness (100 nm) of resist are given, with a lower dose level of 600 μC/cm^2. A similar observation, i.e., a close match between the analytic and simulation results, can be made.

One observation to make is that the LER outside the feature ($x > 0$) in Fig. 8(c) increases while it continues to decrease in Figs. 8(a) and 8(b). Given a stochastic exposure distribution, the LER generally depends on two factors, the exposure fluctuation and contrast. A higher exposure contrast makes the LER smaller. On the other hand, ignoring the effect of the exposure contrast, the LER would be larger at a more positive edge location (i.e., further outside or equivalently a longer developing path) since the exposure fluctuation is accumulated over a longer developing path. These factors compete with each other. The LER may increase or decrease outside a feature depending which factor becomes more dominant. That is, the exposure contrast outside the feature in Figs. 8(a) and 8(b) is relatively higher than that in Fig. 8(c).

(a)

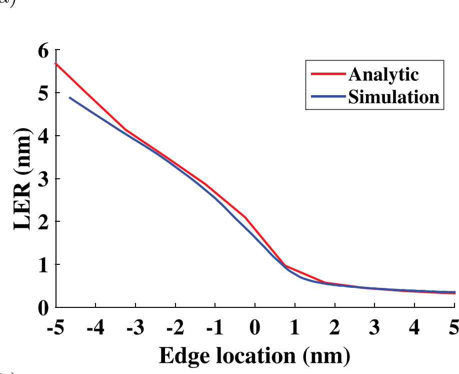

(b)

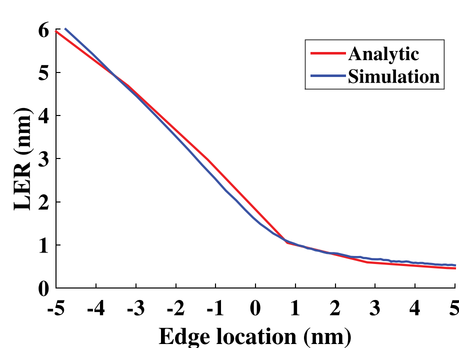

(c)

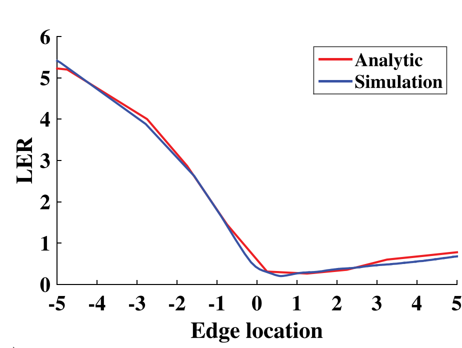

(d)

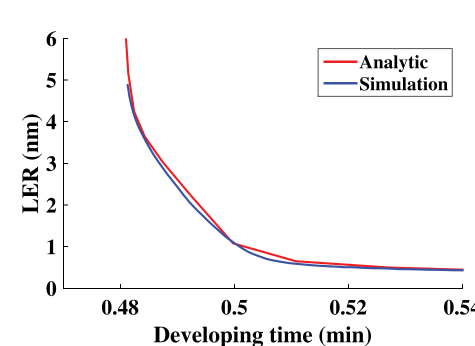

FIG. 8. (Color online) LER estimated by the analytic and simulation methods: (a) 300 nm PMMA on Si, beam energy of 50 keV, dose of 640 μC/cm^2, (b) 300 nm PMMA on Si, beam energy of 30 keV, dose of 640 μC/cm^2, (c) 100 nm PMMA on Si, beam energy of 50 keV, dose of 600 μC/cm^2, and (d) 300 nm PMMA on Si, beam energy of 50 keV, dose of 640 μC/cm^2.

Redistribution subject to AVS license or copyright; see http://scitation.aip.org/termsconditions. Download to IP: 131.204.21.179 On: Thu, 19 Nov 2015 16:00:59

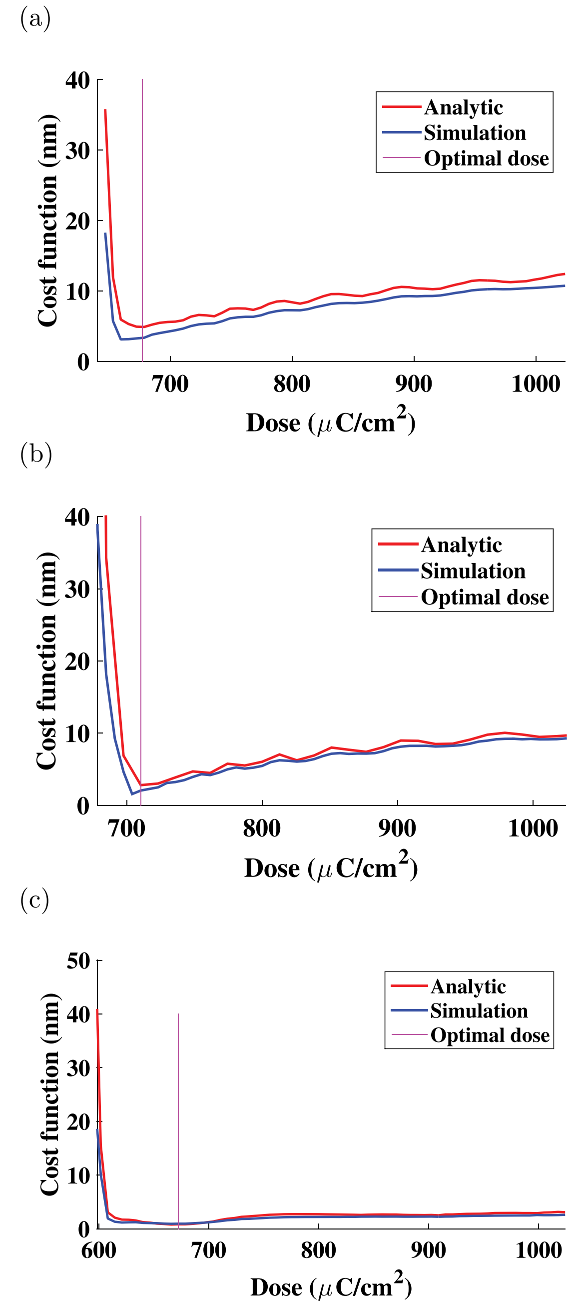

FIG. 9. (Color online) Minimization results (minimization of the cost function with respect to the dose) by the analytic and simulation methods: (a) 300 nm PMMA on Si, beam energy of 50 keV, developing time of 50 s, (b) 300 nm PMMA on Si, beam energy of 30 keV, developing time of 20 s, and (c) 100 nm PMMA on Si, beam energy of 50 keV, developing time of 10 s. The optimal dose computed by the analytic method is indicated by the vertical line in the graphs.

For an edge location, the developing time is the same for both the analytic method and simulation. In Fig. 8(d), the LER is plotted as a function of developing time for both analytic model and simulation [for the case of Fig. 8(a)].

The cost function is evaluated by both the analytic and simulation methods, and the optimal dose, which minimizes the cost function, is computed by the analytic method, i.e., evaluating Eq. (24). The analytic minimization of the LER and CD error by controlling the dose is compared with the minimization by the simulation method with a fixed developing time. In Fig. 9(a), the results for the resist thickness of 300 nm and the beam energy of 50 keV are provided. The cost function evaluated by the analytic method is well matched with that by the simulation method, and the optimal dose obtained by the analytic procedure is very close to the optimal dose by the simulation method. In Figs. 9(b) and 9(c), the results for a lower beam energy of 30 keV and a thinner resist thickness of 100 nm are shown, respectively. It is noted in Fig. 9(c) that the cost function shows a flat portion. When the exposure contrast over the feature edge is high (in general, higher for an upper layer of resist, a thinner resist, a higher beam energy, etc.), the exposure outside (even right outside) a feature is very low. In such a case, the width of developed feature increases very slowly as the dose (or developing time) increases, leading to the flat portion of the cost function [see Fig. 9(c)]. One may still use the optimum dose or the lowest dose in the flat portion in practice since the cost function does not vary substantially in that region.

VI. SUMMARY

As the feature size decreases, the LER will eventually become a resolution-limiting factor in e-beam lithography since the LER does not scale with the feature size. Therefore, it is essential to minimize the LER in order to achieve the highest resolution possible by the e-beam lithographic process. The main drawback of a simulation approach for estimating the LER is the intensive computation required. In this study, a new analytic method for estimating the LER and an analytic procedure for minimizing the LER based on the new analytic model are developed as a first step toward reducing the need for the time-consuming simulation and expensive experiment. It has been shown that the results obtained by this analytic approach for estimating and minimizing the LER are closely matched with the simulation results. Though a specific cost function is employed in this study, it should be clear that the analytic methods developed are applicable with any other cost function (as long as it is a linear combination of the CD error and LER). The study reported in this paper focuses on the stochastic variation of the developing rate. Nevertheless, the analytic estimation method and the minimization procedure developed in this study are expected to be applicable even when other factors contributing to the LER are taken into account, by reflecting their direct or equivalent effects in the developing rate. In the future, the analytic model and method will be extended to improve their applicability.

ACKNOWLEDGMENT

This work was supported by a research grant from Samsung Electronics Co., Ltd.

[1]R. Rau, J. McClellan, and T. Drabik, J. Vac. Sci. Technol. B **14**, 2445 (1996).
[2]G. P. Watson, L. A. Fetter, and J. A. Liddle, J. Vac. Sci. Technol. B **15**,2309 (1997).
[3]R. Murali, D. Brown, K. Martin, and J. Meindl, J. Vac. Sci. Technol. B **24**, 2936 (2006).

Redistribution subject to AVS license or copyright; see http://scitation.aip.org/termsconditions. Download to IP: 131.204.21.179 On: Thu, 19 Nov 2015 16:00:59

[4]Q. Dai, S.-Y. Lee, S.-H. Lee, B.-G. Kim, and H.-K. Cho, J. Vac. Sci. Technol. B **29**, 06F314 (2011).
[5]H. Eisenmann, T. Waas, and H. Hartmann, J. Vac. Sci. Technol. B **11**, 2741 (1993).
[6]S.-Y. Lee and B. D. Cook, IEEE Trans. Semicond. Manuf. **11**, 108 (1998).
[7]M. Osawa, K. Takahashi, M. Sato, and H. Arimoto, J. Vac. Sci. Technol. B **19**, 2483 (2001).
[8]Q. Dai, S.-Y. Lee, S.-H. Lee, B.-G. Kim, and H.-K. Cho, J. Vac. Sci. Technol. B **30**, 06F307 (2012).
[9]M. Nagase, H. Namatsu, K. Kurihara, K. Iwadate, K. Murase, and T. Makino, Jpn. J. Appl. Phys. **35**, 4166 (1996).
[10]J. Bolten and T. Wahlbrink, Microelectron. Eng. **88**, 1910 (2011).
[11]W. Cho and H. Kim, J. Korean Phys. Soc. **56**, 1767 (2010).
[12]X. Zhao, S.-Y. Lee, J. Choi, S.-H. Lee, I.-K. Shin, and C.-K. Jeon, J. Vac. Sci. Technol. B **32**, 06F505 (2014).
[13]J. A. Croon, G. Storms, S. Winkelmeier, I. Pollentier, M. Ercken, S. Decoutere, W. Sansen, and H. E. Maes, *IEDM02 International Electron Devices Meeting* (2002), pp. 307310.
[14]C. H. Diaz, H. Tao, Y. Ku, A. Yen, and K. Young, IEEE Electron Device Lett. **22**, 287 (2001).
[15]C. A. Mack, Future Fab Int. **34**, 64 (2010).
[16]R. Guo, S.-Y. Lee, J. Choi, S.-H. Lee, I.-K. Shin, C.-U. Jeon, B.-G. Kim, and H.-K. Cho, J. Vac. Sci. Technol. B **31**, 06F408 (2013).
[17]Q. Dai, R. Guo, S.-Y. Lee, J. Choi, S.-H. Lee, I.-K. Shin, C.-U. Jeon, B.-G. Kim, and H.-K. Cho, Microelectron. Eng. **127**, 86 (2014).

Redistribution subject to AVS license or copyright; see http://scitation.aip.org/termsconditions. Download to IP: 131.204.21.179 On: Thu, 19 Nov 2015 16:00:59